

## Permeability upscaling in fractured reservoirs using different optimized mother wavelets at each level

R. Vahedi<sup>1\*</sup>, B. Tokhmechi<sup>1</sup> and M. Koneshloo<sup>2</sup>

1. School of Mining, Petroleum & Geophysics Engineering, Shahrood University of Technology, Shahrood, Iran

2. Department of Chemical and Petroleum Engineering, University of Wyoming, Laramie, USA

Received 21 July 2013; received in revised form 11 October 2015; accepted 19 December 2015

\*Corresponding author: [raziyh.vahedi@gmail.com](mailto:raziyh.vahedi@gmail.com) (R. Vahedi).

### Abstract

We use a multi-resolution analysis based on a wavelet transform to upscale a 3D fractured reservoir. This paper describes a 3D, single-phase, and black-oil geological model (GM) that is used to simulate naturally-fractured reservoirs. The absolute permeability and porosity of GM is upscaled by all the possible combinations of Haar, Bior1.3, and Db4 wavelets in three levels of coarsening. The applied upscaling method creates a non-uniform computational grid, which preserves its resolved structure in the near-well zones as well as in the high-permeability sectors but the data are scaled up in the other regions. To demonstrate the accuracy and efficiency of the method, the values for the oil production rate, mean reservoir pressure, water cut, and total amount of water production are studied, and their mean error is estimated for the upscaled models. Finally, the optimized model is selected based on the computation time and accuracy value.

**Keywords:** 3D Simulation, Fractured Reservoir, Upscaling, Wavelet Transform, Optimization.

### 1. Introduction

Geological models (GMs) are often generated on a fine-scale model to represent the geological variations, especially in the vertical direction, where the data has a more resolution. Flow simulation in such models entails highly intensive computations [1-4]. A typical flow simulator handles around  $10^5$  to  $10^6$  cells, while a GM typically contains around  $10^7$  to  $10^8$  cells. As an essential component of a reservoir management, we have to evaluate the risk and uncertainty of the model responses, and thus we need to run thousands of such simulations [5,6]. Therefore, it is necessary to upscale the properties of the GM grid blocks to a coarsened grid that can be used in a reservoir simulation with an economical amount of computation time, while ensuring that the predictions resulting from the coarse model is close enough to the reference fine-scale model.

Upscaling is carried out for the simulation of a reservoir with a single-phase or multi-phase flow. Single-phase upscaling is concerned with upscaling absolute permeability, while multi-

phase upscaling deals with upscaling absolute and relative permeabilities [5,7].

For a single-phase flow, upscaling techniques can be divided into several classifications based on the derivation method performed (analytical or numerical), geological model employed (deterministic versus stochastic), and dependence on the boundary conditions (local/extended-local, global/quasi-global, local/global) [8].

In this work we used a different upscaling method to simulate a single-phase and fractured reservoir. This method is based on the wavelet transformation (WT). While most hydrocarbon reservoirs in Iran are naturally-fractured, this type of reservoir is selected for simulation.

In 1994, wavelet analysis was used in petroleum engineering to enhance the rock property images and denoise the measurement of rock properties [9]. Also in the same year, WT was used in environmental engineering to down sample the absolute permeability [10]. In 1996, Panda et al. applied WTs to 1D and 2D upscalings of the

permeability data [11]. Later, the wavelet-based upscaling of the single-phase permeabilities was developed [12-15]. The method is a multi-resolution or multi-scale approach, which acts as an automatic grid generator at different and relevant length scales that are incorporated in GM. The accuracy and computational efficiency of this technique have been demonstrated by applying it to the simulation of two-phase flow models of heterogeneous reservoirs [16,17], and the simulation of unstable miscible displacements [14]. In the mentioned research works, only one kind of wavelet function (WF) (Haar or Db4) has been applied for upscaling. We aimed to investigate the effect of using different WFs at each upscaling level. All the possible combinations of Haar, Db4, and Bior 1.3 functions were used for the three level upscaling of GM.

In this paper, we present a wavelet analysis, and then the important properties of the WTs used are described. In section 3, the technical properties of GM and the methodology of the wavelet-based upscaling are presented, and then the results of nine upscaled models are compared to the results of the initial GM, and subsequently, the performance of the upscaled models are discussed. Conclusion and selection of the best model are made based on the errors of the four responses of the upscaled models (oil production rate, water cut, mean reservoir pressure, and total water production) by considering their simulation times.

## 2. Wavelet analysis

### 2.1. Wavelet definition

In 1982, a French geophysicist, Jean Morlet, introduced the concept of a 'wavelet' that means a small wave [18].

In other words, a wavelet is an oscillation function that decays quickly. Mathematically, wavelet is a tool that represents type (1) of a large class of functions  $f$ .

$$f(x) = \sum_{n=0}^{\infty} a_n f_n(x) \tag{1}$$

Several researchers have explained the construction and applications of wavelets [19-21]. Indeed, wavelets are a family of functions that are constructed from the translations and dilations of a single function called the "mother wavelet"  $\Psi_{ab}(X)$ . The wavelets are defined as:

$$\Psi_{ab}(X) = \frac{1}{a^{\frac{d}{2}}} \psi\left[\left(\frac{X-b}{a}\right)\right] \tag{2}$$

where  $a > 0$ ,  $-\infty < b < +\infty$ , and  $d$  is the dimension of the system. The parameter  $a$  is the scaling parameter, and the parameter  $b$  is the translation parameter. By setting  $|a|$ , the dilation can be changed. Therefore, for high frequencies,  $\Psi_{ab}(x)$ 's are narrow, whereas for low frequencies,  $\Psi_{ab}(x)$ 's are wide.

The mathematical condition for a mother wavelet functions is:

$$\int_{-\infty}^{+\infty} |\Psi(X)| dX = 0 \tag{3}$$

### 2.2. Wavelet transformation

The important difference between a wavelet transformation (WT) and a Fourier analysis is that a Fourier transform (FT) is localized in frequency but a WT is localized both in time and frequency, and this property makes wavelets more practical in comparison to FTs [22]. A WT is defined as a convolution of a given function  $f(x)$  with a wavelet function. Thus a WT of a spatially varying single-phase permeability  $K(X)$  is defined as:

$$D(a,b) = \int_{-\infty}^{+\infty} K(X) \Psi_{ab}(X) dX = \frac{1}{a^{\frac{d}{2}}} \int_{-\infty}^{+\infty} K(X) \psi\left[\frac{X-b}{a}\right] dX \tag{4}$$

$D(a,b)$  is also called the wavelet detail coefficient of function  $K(X)$  that contains information only about the difference or contrast between two approximations of the same function at two successive length scales. When a given wavelet is convoluted with  $K(X)$ , the magnitude of the results is a measure of the match between the wavelet and  $K(X)$ .

For analyzing the discrete data, the discrete wavelet transform (DWT) can be used. This requires discretizing the scaling parameter "a" and location or translation of wavelet parameter "b" based on following definitions:

$$A = a_0^L \text{ and } b = ka_0^L \tag{5}$$

where  $L$  is the scaling level, and  $k$  is an integer ( $nb_0 = k$ ). Basic analysis of the wavelet on a discrete data can be written by selecting  $a_0 = 2$  and  $b_0 = 1$ . Thus in a 1D system, DWT is:

$$D_{L,k} = 2 \frac{-L}{2} \int_{-\infty}^{+\infty} (2^{-L} x - k) K(x) dx \quad (6)$$

The most accurate approximation of  $K(X)$  at a fixed scale is given by another function called the scaling function,  $\varphi(x)$ . In a 1D system, the scaling coefficient approximation in  $k$  translation and  $L$  scale is defined by equation (7).

$$S_{L,k} = \int_{-\infty}^{+\infty} K(x) \varphi_{L,k}(x) dx \quad (7)$$

where  $\varphi(x)$  is orthogonal to  $\psi(x)$ . Eqs. (6) and (7) in the 2D and 3D systems can be defined in a straightforward manner. The wavelet and scaling functions can be fully defined by their coefficients (Eqs. (8) and (9)). The lower the number of coefficients, the more localized the support will be.

$$\varphi(X) = \sum_{K=-\infty}^{+\infty} h_K \varphi(2X - K) \quad (8)$$

$$\Psi(X) = \sum_{K=-\infty}^{+\infty} g_K \psi(2X - K) \quad (9)$$

where  $h_k$  is called the scaling filter coefficient and  $g_k$  is the detailed filter coefficient. The scaling filter coefficients are related to  $g_k$  by  $g_k = (-1)^k h_{M-1-k}$  by  $k = 0, 1, 2, \dots, M-1$ . The amount of  $M$  is dependent on WF. The mentioned discussion is only limited to a 1D dataset; it can

be extended to 2D or 3D datasets as well. Mallat presented a simple extension of a 1D multi-resolution analysis to a 2D one [23,24]. In a 2D analysis, there is one scaling function:

$$\varphi_{L,k_1,k_2} = \varphi_{L,k_1}(x) \varphi_{L,k_2}(y) \quad (10)$$

and there are three 2D WFs:

$$\Psi_{L,k_1,k_2}^{(1)}(x, y) = \varphi_{L,k_1}(x) \Psi_{L,k_2}(y) \quad (11)$$

$$\Psi_{L,k_1,k_2}^{(2)}(x, y) = \Psi_{L,k_1}(x) \varphi_{L,k_2}(y) \quad (12)$$

$$\Psi_{L,k_1,k_2}^{(3)}(x, y) = \Psi_{L,k_1}(x) \Psi_{L,k_2}(y) \quad (13)$$

The extension of a 2D analysis into a 3D one is possible using the 1D decomposition technique recursively. The number of all functions (wavelet and scaling function) for each higher dimension increases by a factor of 2. The relationship between the number of all of these functions and the spatial dimension is  $2^d$ , where  $d$  indicates the number of dimensions. Therefore, a total of eight functions for 3D upscaling is needed (Figure 1). In a 3D upscaling, a 3D tensor is directly defined by construction the 2D tensorial case [25,26].

The WFs used in this study were Haar, Db4, and Bior1.3. Their filter coefficients are represented in Table 1.

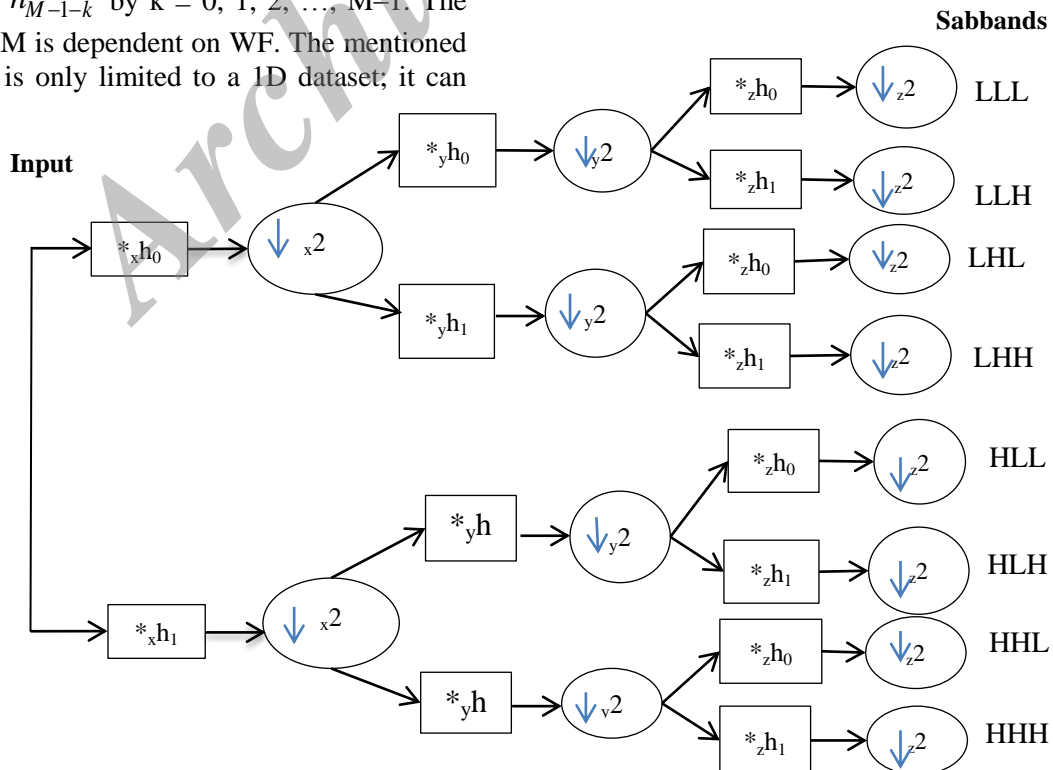


Figure 1. Process of 3D wavelet transforms.

**Table 1. Coefficients of wavelets and scaling functions for Haar, Db4, and Bior1.3 wavelet functions.**

Low-pass coefficients	Wavelet types			High-pass coefficients	Wavelet types		
	Haar	Db4	Bior1.3		Haar	Db4	Bior1.3
$h_0$	0.7071	0.4829	-0.0883	$g_0$	-0.7071	-0.1294	0
$h_1$	0.7071	0.8365	0.0883	$g_1$	0.7071	-0.2241	0
$h_2$		0.2241	0.7071	$g_2$		0.8365	-0.7071
$h_3$		-0.1294	0.7071	$g_3$		-0.4829	0.7071
$h_4$			0.0883	$g_4$			0
$h_5$			-0.0883	$g_5$			0

### 3. Materials and method

#### 3.1. Geological model

To imitate a fractured reservoir, a geological model (GM) was generated by combining a homogeneous background and the simulated fractured zones. The model was represented by a regular Cartesian grid. Its dimensions were  $256 \times 256 \times 256$  m. The fine-scale (geological) model contained  $64 \times 64 \times 64$  blocks. The data related to the absolute permeability, porosity, and geometry of the reservoir was numerically generated. The permeability and porosity values in each node were produced by a linear combination of two models. The first model consisted of the values generated using the sequential Gaussian simulation (SGS) method as the background or the property of intact rock (for a detailed study of the method, refers to [27]), and the second model was constructed to imitate the fractures. In the simulated model, the porosity varied between 5% and 30%, and the distribution of permeability varied between 350 and 1660 md. To simplify the model, the permeability was assumed isotropic ( $k_x = k_y = k_z$ ). The top of the reservoir was at a depth of 790 m. To allow maximum flexibility in selecting the upscaled grids, the model had no fault.

#### 3.2. Technical parameters of GM

In this section, the properties of the reservoir fluids (water and dead oil) and the two wells (injection and production wells) used in our research work are described. The properties of the fluids are listed in Table 2.

In Table 2, B is the expansion coefficient, C is the compressibility, and  $\mu$  represents the fluid viscosity. The fluid properties were taken from an Iranian oil reservoir.

The injection and production wells were both assumed to be drilled vertically and perforated along the synthetic pay zones. The initial pressure of the reservoir was set at 3480 bar, and the simulation period was 600 days. The bottom-hole pressure in the injection well (in block (59, 59))

was 3700 bar, while in the production well (in block (9, 9)), it was estimated to be 3200 bar and assumed to be constant. The described GM was simulated by the Eclipse® simulator.

**Table 2. Dead oil and water properties used for flow simulation in GM and nine upscaled models.**

Parameter	Symbol	Assumed or default value
Expansion coefficient	$B_o$	1
	$B_w$	1.01
Pressure	$P_o$	700 psi
Viscosity	$\mu_o$	5 cp
	$\mu_w$	1 cp
Compressibility	$C_o$	$4 \times 10^{-6}$ psi <sup>-1</sup>
	$C_w$	$3 \times 10^{-6}$ psi <sup>-1</sup>

#### 3.3. Methodology of upscaling using WT

GM was represented by a square grid, in which  $K(\mathbf{x})$  represented the permeability of a grid block of the GM with its center at  $\mathbf{x}$ . To begin the upscaling of GM, firstly, DWT of  $K(\mathbf{x})$  was computed. There were eight wavelet coefficients associated with DWT at every block centered at  $\mathbf{x} = (k_1, k_2, k_3)$ , given (refer to Figure 1) by:

$$S_{L(k_1, k_2, k_3)} = \int_{\Omega} K(x, y, z) \phi_{L, k_1, k_2, k_3}(x, y, z) dx dy dz \quad (14)$$

$$D_{L(k_1, k_2, k_3)}^l = \int_{\Omega} K(x, y, z) \Psi_{L, k_1, k_2, k_3}^l(x, y, z) dx dy dz \quad (15)$$

where  $\Omega$  is the domain of the system, and L is the upscaling level.  $S_{L, k_1, k_2, k_3}$  contains information about  $K(\mathbf{X})$  at a fixed scale of the grid, whereas  $D_{L(k_1, k_2, k_3)}^l$  represents a measure of the contrast between the permeability  $K(\mathbf{X})$  in coarser scale

and those of the block neighbors in the previous finer scale grid with  $l=1, 2, 3, \dots$  and 7. In other words, in a 3D upscaling,  $D_{L(k_1, k_2, k_3)}^l$  measures the contrast or difference in K between the blocks in the x, y, and z directions and the xy, xz, yz, and xyz diagonal directions.

For the coarsening process, two thresholds  $\mathcal{E}_s$  and  $\mathcal{E}_d$  were introduced.  $\mathcal{E}_s$  and  $\mathcal{E}_d$  were set as a fraction of the largest values of wavelet scale and wavelet detail coefficients throughout the grid for the first to the third level of upscaling. In this work, for all levels,  $\mathcal{E}_s$  and  $\mathcal{E}_d$  were set 0.8, 0.7, and 0.6 ( $\mathcal{E}_s = \mathcal{E}_d$  at each level). Indeed, as mentioned in Section 2.2 and Figure 1, at each level of 3D upscaling, there are one matrix of wavelet scale coefficients and 7 matrices of wavelet detail coefficients (in the x, y, and z directions and the xy, xz, yz, and xyz diagonal directions). Among these eight matrices, the matrix of wavelet detail coefficients at xyz diagonal directions and the wavelet scale coefficients were used in upscaling. The wavelet detail coefficients at the xyz diagonal directions had the main details of data. Indeed, the scale coefficient matrix elements are the values of a given block's permeability, and the detail coefficient matrix elements measure the difference or contrast between the permeability of the neighboring blocks. During upscaling, the fraction of the largest value for the scale coefficients matrix elements (FS) is defined using  $\mathcal{E}_s$ , and similarly, for the fraction of the largest value of detail coefficient matrix elements (FD) is determined using  $\mathcal{E}_d$ . Then the scale coefficient and detail coefficient of each block (the elements of matrices) were examined as follow:

- If the scale coefficient of each block ( $S_{L, k_1, k_2, k_3}$ ) is larger than FS, implying that the block's value (this value is permeability)

is large enough, thus it is left intact, and we move to the next block to examine its grid.

- If  $S_{L, k_1, k_2, k_3} < FS$ , the associated detail coefficient xyz diagonal direction ( $D_{L(k_1, k_2, k_3)}^l$ ) is examined; if it is smaller than FD, then that block is set to the coefficient scale value ( $S_{L, k_1, k_2, k_3}$ ) for permeability value. This means that the neighbour of the block is centred at  $(k_x, k_y, k_z)$  corresponding to the direction  $l$ , which, in a finer-scale grid, is one block (or one diagonal block) away from it. Thus the two blocks might be merged to form one grid with twice as large [16, 28-30].
- If  $S_{L, k_1, k_2, k_3} < FS$  and  $D_{L(k_1, k_2, k_3)}^l > FD$ , then this condition indicates that there is a large contrast between the permeabilities of the two neighboring blocks in two successive scales. These zones are important in a reservoir simulation, and must be fine-scaled.

Similarly, all the scales and detail coefficients were examined.

The A C++ code was written to handle all these steps, and to generate the output as an importable file to the Eclipse simulator. This code created a list of block properties, which contained the coordinate of the blocks to be upscaled and their new permeability values resulted by applying different types of DWT on the K(X) of the previous finer model at each level on a regular grid. This means that for our nine generated models, the coordinate and the new permeability values were listed in a file but the grids were not merged. Eclipse simulator merged the specified blocks and set equivalent permeability values as the permeability of the merged blocks.

As the Eclipse® simulator uses the simple averaging method for upscaling, and the averaging is not a valid approach for heterogeneous reservoirs, in this way, we forced the Eclipse® simulator to average the result of WT on grid blocks of reservoir instead of averaging the initial values. Figure 2 shows the geological (fine-scale) model, and Figure 3 shows a sample of a model upscaled by the mentioned method.

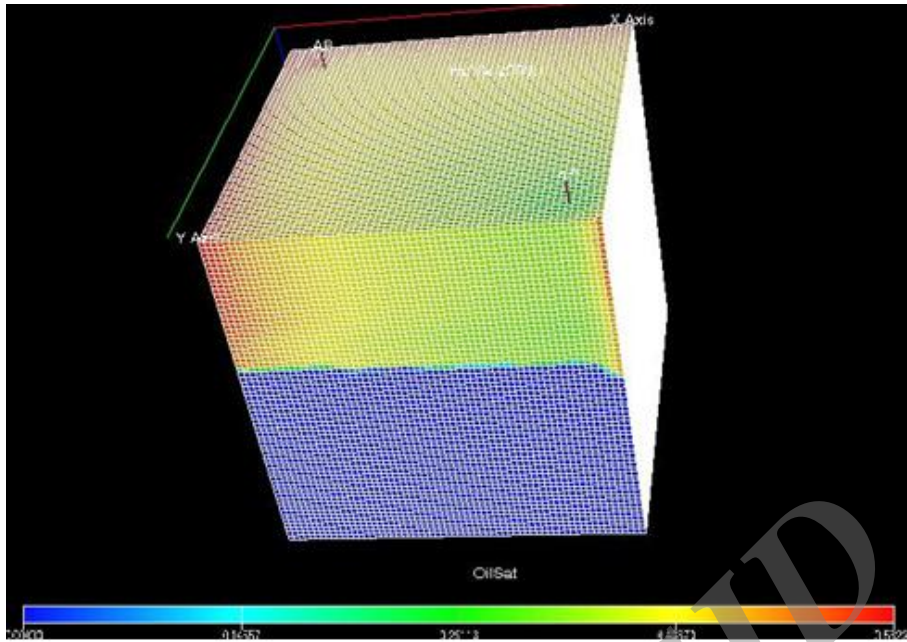


Figure 2. Fine-scale (geological) model simulated in this work.

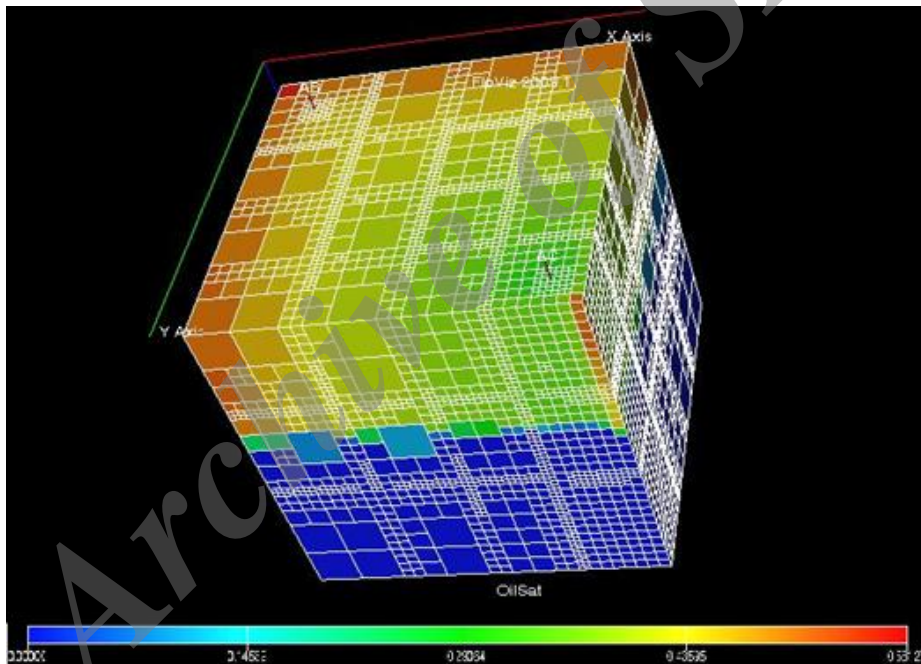


Figure 3. A sample of upscaled model generated by WT upscaling in this work.

#### 4. Results

It is worthy to note that the largest variations in the oil saturation, permeability, and field pressure occur in the near-well regions. Thus the structure of the grid around the (injection and/or production) wells is important. Due to the high variation arising from the fluid flow, the space surrounding the injection well, named M, was a  $8 \times 8$  window that was not coarsened; also a  $6 \times 6$  window surrounding the production well, named N, remained fine likewise.

Also the areas with high permeability changes (such as those around the fractures) and high

permeability values (fractures) remained fine-scaled because these areas contained important features. The areas with high permeability values were the main flow paths, which contained decisive information. These zones were detected by WT. Finally, we had a non-uniformly upscaled structure as the model.

For the sake of simplicity, here we used abbreviations for the combinations. For example, HDB stands for an upscaled model generated by upscaling using the Haar wavelet function at the first level, Db4 at the second one, and Bior1.3 at

the third one. The results of the fine model (GM) and its equivalent coarsened models using the same WT for all the steps (HHH, DDD, and BBB) were represented and compared in Figures 4-6, respectively, for the oil production rate, mean reservoir pressure, and water cut (which is the ratio of the water produced compared to the volume of the total liquids produced in the reservoir). Figures 7-9 show the results of other models. Now we describe the results obtained for each parameter in detail.

#### 4.1. Oil production rate

The accuracy value (error) varies according to the WFs used for different upscaled models. As clearly seen in Figure 4, the models upscaled using Bior1.3 at the first or second level had a larger error than the other models, except for the BBB model. The other models upscaled by Bior 1.3 at the first or second level had a relatively low simulation time. Model HHH had the smallest error and the smallest value of error standard deviation but the highest value of computation time. In average, the models upscaled by the Haar wavelet at the first step had a better result than the model upscaled by Db4.

#### 4.2. Water cut

For the water cut, we had similar results, and distinction between the error of the models upscaled by Bior1.3 at the first step and the other

models is obvious (see Figure 5). This difference between the groups (models starting with B, H, and D) is significant ( $p$ -value = 0.02) based on the single factor ANOVA. The HDM model, despite its relatively low simulation time, provided the best results after the HHH model.

#### 4.3. Mean reservoir pressure

The pattern for the model errors for mean reservoir pressure was different from the two previous parameters, and the groups were not easily distinct based on their errors. The error for the HHH model was significantly lower than those for the other models (see Figure 6). The HDB model did not have a good performance in the estimation of the reservoir average pressure.

#### 4.4. Ratio of water produced

Conforming to the other parameters, in average, the model upscaled by Bior1.3 at the first level had a bigger error than the other two models. Among the models upscaled using Db4 and Haar, the model upscaled by the Bior1.3 wavelet at the second level performed worse than the model upscaled by Bior 1.3 at the third level.

Table 3 represents the mean error calculated for the oil production rate, water cut, water production total, mean pressure reservoir, and the required time for simulation of these models compared to the initial GM.

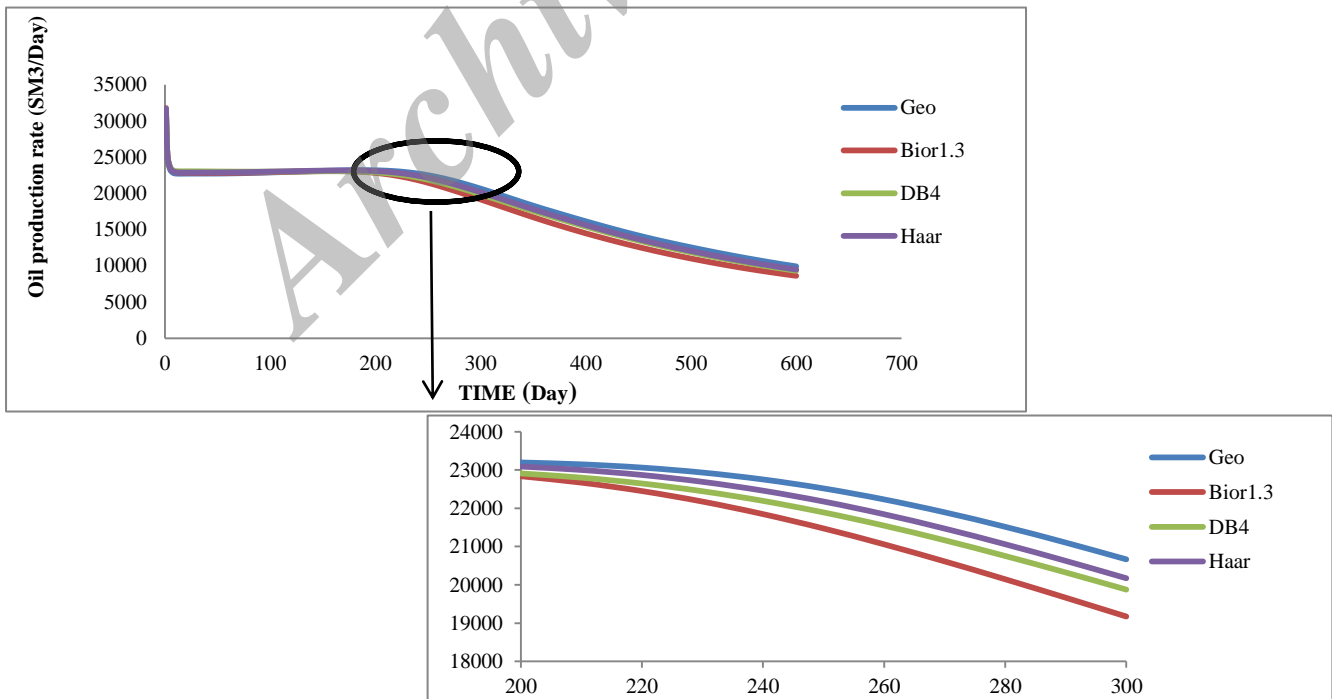


Figure 4. Comparison of oil production rate during simulation time for GM and upscaled models, of which the same WF was used in each level.

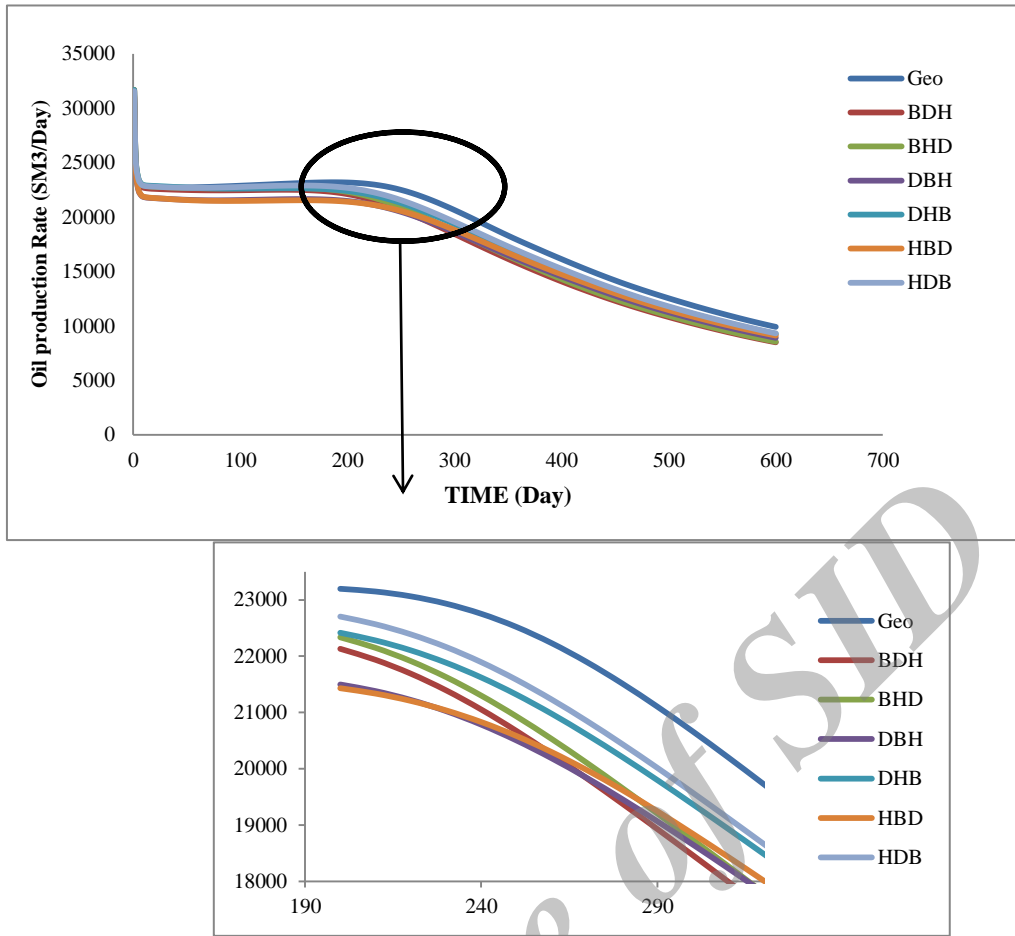


Figure 5. Rate of oil production versus time for GM and other upscaled models.

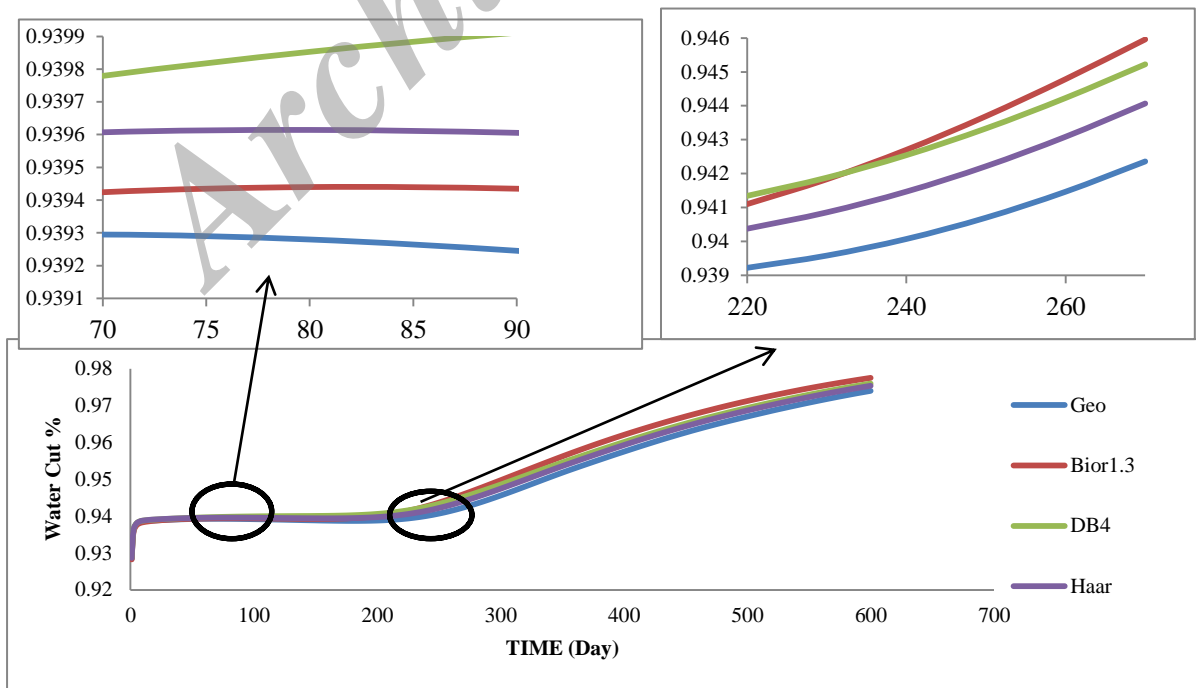


Figure 6. Water cut in GM and upscaled models, of which the same WF was used in each level.



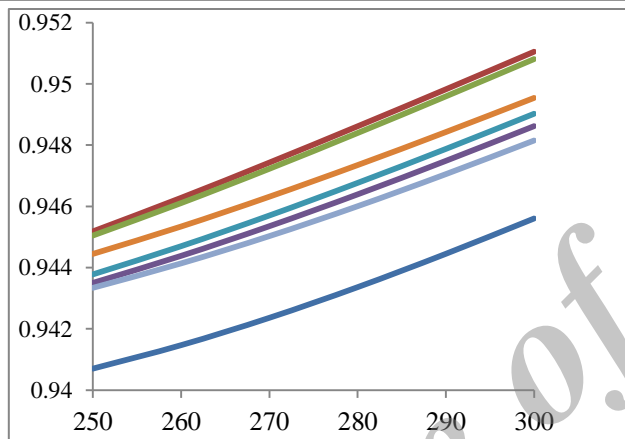
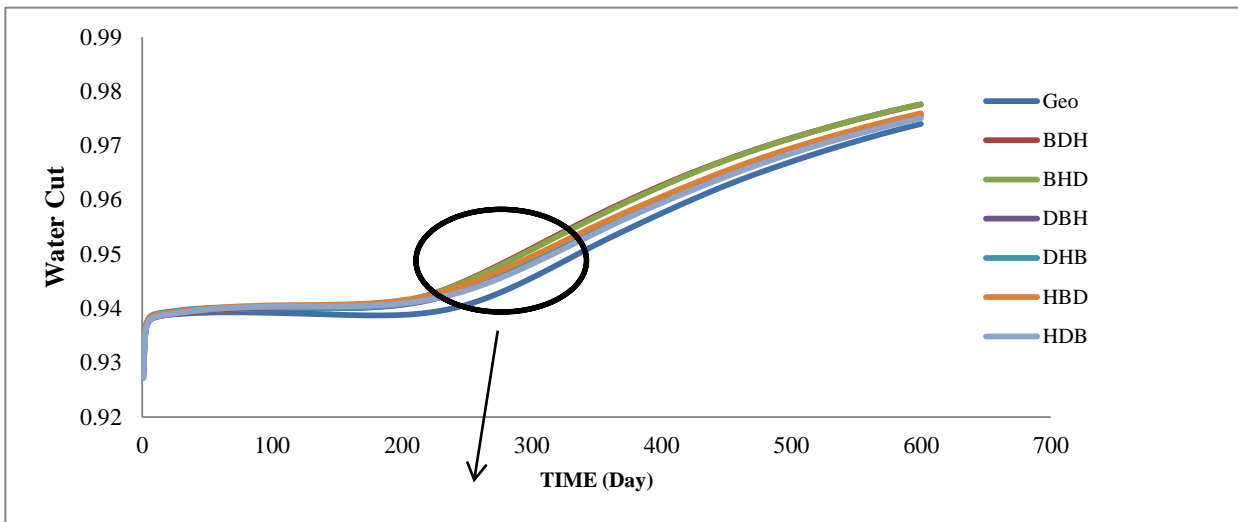


Figure 7. Time-dependence of water cut in GM and other upscaled models.

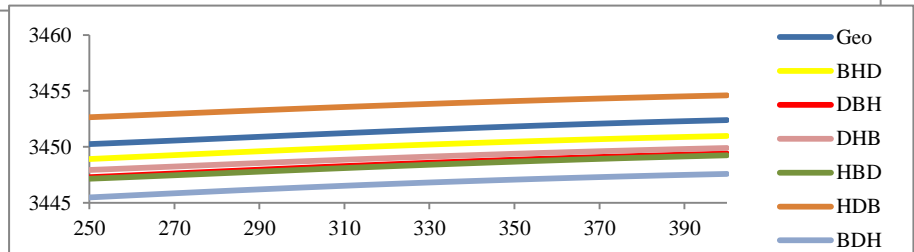
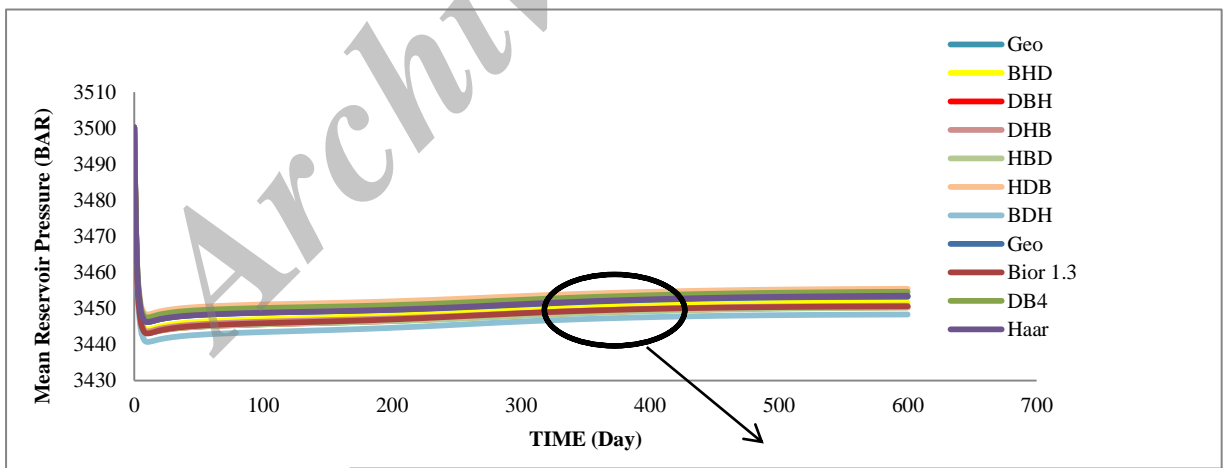


Figure 8. Comparison of mean reservoir pressure in GM and upscaled models.

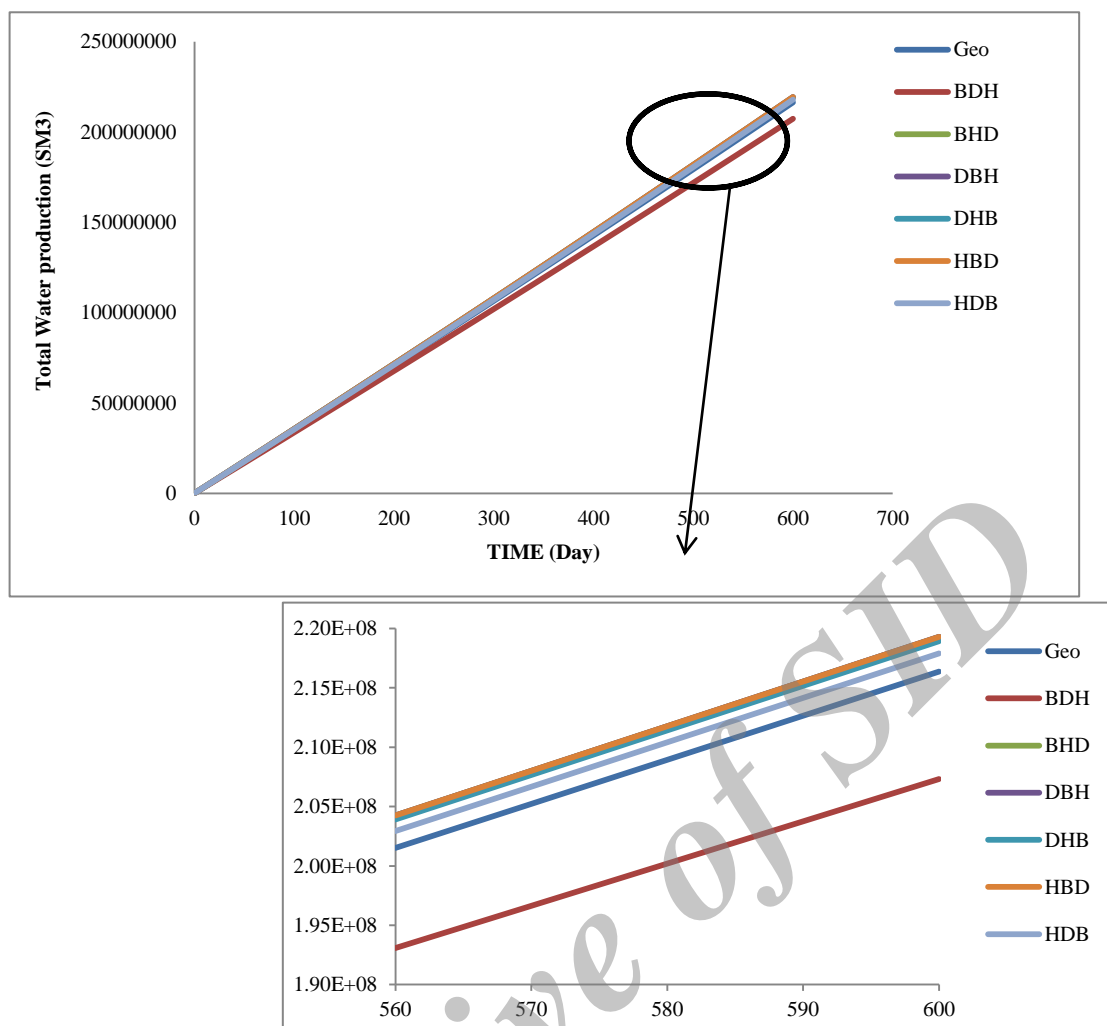


Figure 9. Total water production in GM and other upscaled models.

Table 3. Mean error and simulation time for upscaled models.

Models name	Wavelet type at levels 1 to 3 of upscaling	Mean errors for parameters of ... (%)				Simulation time (Second)
		Oil production rate (SM <sup>3</sup> /Day)	Water cut	Mean pressure (BAR)	Total water production (SM <sup>3</sup> )	
BDH	Bior1.3, Db4, Haar	7.836	0.323	0.141	4.1713	241
DBH	Db4, Bior1.3, Haar	7.916	0.183	0.085	1.2487	239
HHH	Haar, Haar, Haar	2.0426	0.12	0.00315	0.2126	554
BHD	Bior1.3, Haar, Db4	6.985	0.318	0.045	1.2772	221
HBD	Haar, Bior1.3, Db4	7.225	0.236	0.087	1.2772	248
DDD	DB4,Db4, Db4	3.0097	0.186421	0.03538	1.16	431
DHB	Db4, Haar, Bior1.3	4.182	0.205	0.0724	0.58	281
HDB	Haar, Db4, Bior1.3	3.487	0.162	0.0621	0.5547	300
BBB	Bior1.3, Bior1.3, Bior1.3	5.8822	0.26175	0.077134	1.83	351

### 5. Discussion

As shown in the previous section, the upscaled HHH model is the most accurate one. It has the minimum value of error for all the simulated parameters but despite its accuracy, the simulation time of the model is very high. After the HHH model, the DDD model has the highest simulation

time. It estimates the oil production rate and mean pressure better than the other models (except for HHH). Generally, among the nine upscaled models, the accuracy of HHH model > DDD model > BBB model, and the simulation time for HHH model > DDD model > BBB model.

The HHH and DDD models, due to high simulation times, and BBB model, due to low accuracy, are not the optimized models for the reservoir simulation. Production rate (OPR) can be estimated with a good accuracy by the HDB and DHB models (see Table 3 and Figures 4 and 5). The HDB model has a smaller error than the DDD model for the estimation of water cut and water production rate, while its simulation time is 35% less than the needed time by the DDD model.

## 6. Conclusions

Wavelet-based upscaling method is one of the successful methods applied to upscale heterogeneous GMs or fractured reservoirs, and leads to an important reduction in the computational time with a reasonable precision. As shown in this paper, the method is accurate and efficient. We hypothesized that the wavelet transform usage depended on the structure and heterogeneity of the field, and, as the structure and heterogeneity of the model are scale-dependent features, thus using the same class of WT is not always suitable. The Functions that were used in this work were Haar, Db4, and Bior 1.3. Nine upscaled models were generated using a combination of these three functions at three levels of upscaling. The accuracies of the oil production rate, water cut, average reservoir pressure, total water production, and simulation time were evaluated.

The results of this study showed that selecting the functions with larger number of coefficients for the first level of scaling up, as Bior 1.3, reduced the model's flow simulation time but the error of the model increased. On other hand, using the functions having a smaller number of coefficient in the first level of upscaling (Haar) led to a higher simulation time, while the error of the model remained small enough. Thus there is an inverse relation between the calculation time and the model's error. As the Haar WT keeps more details of the model, we suggest using this function for the first level of scaling up, and then in the other levels, other wavelet transforms can be used to speed up the simulation time. The results of our model confirms this idea, as shown using the Haar, Db4, and Bior 1.3 wavelet functions, respectively, for the 1<sup>st</sup>, 2<sup>nd</sup>, and 3<sup>rd</sup> levels of upscaling or coarsening.

## References

[1]. Peaceman, D.W. (1977). Fundamentals of Numerical Reservoir Simulations, Elsevier Science, New York, 176 P.

[2]. Aziz, K. and Settari, A. (1979). Petroleum Reservoir Simulation, Applied Sci. Publishers, London, 476 P.

[3]. Thomas, C.W. (1982). Principles of Hydrocarbon Reservoir Simulation, International Human Resources Development Corporation, Boston, 207 P.

[4]. Sahimi, M. (1995). Flow and Transport in Porous Media and Fractured Rock, Second Revised and Enlarged Edition, Wiley-VCH, Weinheim, New York, 718 P.

[5]. Durlofsky, L.J. (2003). Up scaling of Geocellular models for reservoir flow simulation: A Review of Recent Progress, 7 the International Forum on Reservoir Simulation, Buhl/ Baden- Baden, Germany, 23-27 June.

[6]. Durlofsky, L.J. (2005). Upscaling and gridding of fine scale geological models for flow simulation. 8th International Forum on Reservoir Simulation Iles Borromees, Stresa, Italy.

[7]. Noorbakhsh, S., Rasaei, M.R., Heydarian, A. and Behnaman, H. (2014). Single-phase Near-well Permeability Upscaling and Productivity Index Calculation Methods, Iranian Journal of Oil & Gas Science and Technology. 3 (4): 55-66.

[8]. Babaei, M. and King, P.R. (2011). Upscaling reservoir simulation using multilevel operator coarsening, Internatinal conference on water resources, Imperial College London, Barcelona.

[9]. Panda, M.N. (1994). A Forward Modeling of the Interwell Properties in Eolian Deposits. Ph.D. dissertation. University of Michigan.

[10]. Brewer, K.E. and Wheatcraft, S.W. (1994). Including multi-scale information in the characterization of hydraulic conductivity distributions, In: Foufoula-Georgiou, E. and Kumar, P. (Eds), Wavelets in Geophysics. 4: 213-248.

[11]. Panda, M.N., Mosher, C. and Chopra, A.K. (1996). Application of WTs to reservoir data analysis and scaling, SPE Annual Technical Conference and Exhibition, Denver, Colorado, 6-9 October.

[12]. Mehrabi, A.R. and Sahimi, M. (1997). coarsening of heterogeneous media: Application of wavelets. Phys. Rev. Lett. 79: 4385-4388.

[13]. Ebrahimi, F. and Sahimi, M. (2002). Multiresolution wavelet coarsening and analysis of transport in heterogeneous media. Physic A. 316: 160-188.

[14]. Ebrahimi, F. and Sahimi, M. (2004). Multiresolution wavelet scale up of unstable miscible displacements in flow through porous media. Trans. Porous Med. 57: 75-102.

[15]. Ebrahimi, F. and Sahimi, M. (2006). Grid coarsening, simulation of transport processes in, and

scale-up of heterogeneous media: Application of multiresolution WTations. *Mech. Mater.* 38: 772-785.

[16]. Sahimi, M., Rasaei, M.R., Ebrahimi, F. and Haghghi, M. (2005). Up scaling of Unstable Miscible Displacements and Multiphase Flow Using Multiresolution WTation, SPE Reservoir Simulation Symposium, The Woodlands, Texas, 31 January-2 February.

[17]. Lee, S.H., Wang, X., Zhou, H. and Tchelepi, H.A. (2009). Dynamic Up scaling of Multiphase Flow in Porous Media via Adaptive Reconstruction of Fine Scale Variables, SPE Reservoir Simulation Symposium, The Woodlands, Texas, 2-4 February.

[18]. Sifuzzaman, M. and Islam, M.R. (2009). Application of Wavelet Transform and its Advantages Compared to Fourier Transform, *Journal of Physical Sciences.* 13: 121-134.

[19]. Daubechies, I. (1992). Ten lectures on wavelets, Society for Industrial and Applied Mathematics, USA, 357 P.

[20]. Mallat, S.G. (1989). A Theory for Multi-resolution Signal Decomposition, The Wavelet Representation. *IEEE Transactions on Pattern Analysis and Machine Intelligence.* 11: 674-693.

[21]. Vetterli, M. and Herley, C. (1992). Wavelet Filter Banks: Theory and Design. *IEEE Transactions on Signal Processing.* 40: 2207-2232.

[22]. Graps, A. (1995). An Introduction to Wavelets. *IEEE Computational Science and Engineering.*

[23]. Mallat, S.G. (1989). Multifrequency Channel Decomposition of Images and Wavelet Models. *IEEE*

*Transactions on Acoustics, Speech and Signal Processing.* 37: 2091-2093.

[24]. Mallat, S.G. and Hwang, W.L. (1992). Singularity Detection and Processing with Wavelets. *IEEE Transactions on Information Theory.* 38: 617-643.

[25]. Jansen, F.E. (1996). Reservoir Description from Production Data. Ph.D Dissertation, The University of Tulsa.

[26]. Jansen, F.E. and Kelkar, M.G. (1998). Upscaling of Reservoir Properties Using Wavelets, SPE India Oil and Gas Conference and Exhibition, New Delhi, India, 17-19 February.

[27]. Chiles, J.P. and Delfiner, P. (1999). Geostatistics: Modeling Spatial Uncertainty, Wiley-Interscience, USA, 734 P.

[28]. Sahimi, M., Darvishi, R., Haghghi, M. and Rasaei, M.R. (2009). Upscaled Unstructured Computational Grids for Efficient Simulation of Flow in Fractured Porous Media. *Transp Porous Med.* 83: 195-218.

[29]. Rasaei, M.R. and Sahimi, M. (2008). Upscaling and Simulation of Waterflooding in Heterogeneous Reservoirs Using WTations: Application to the SPE-10 Model. *Transp. Porous Med.* 72: 311-338.

[30]. Rasaei, M.R. and Sahimi, M. (2008). Up scaling of the permeability by multiscale WTations and simulation of multiphase flows in heterogeneous porous media. *Springer link.com, ComputeGeosci.* 13:187-214

## افزایش مقیاس تراوایی در مخازن شکافدار با استفاده از توابع موجک مادر متفاوت و بهینه در هر مرحله از افزایش مقیاس

راضیه واحدی<sup>۱\*</sup>، بهزاد تخم‌چی<sup>۱</sup> و محمد کنشلو<sup>۲</sup>

۱- دانشکده مهندسی معدن، نفت و ژئوفیزیک، دانشگاه صنعتی شاهرود، ایران

۲- دانشکده مهندسی شیمی و نفت، دانشگاه ویومینگ، لارامیا، آمریکا

ارسال ۲۰۱۳/۷/۲۱، پذیرش ۲۰۱۵/۱۲/۱۹

\* نویسنده مسئول مکاتبات: razieh.vahedi@gmail.com

### چکیده:

در این مقاله از خاصیت آنالیز چند تفکیکی توابع موجک برای افزایش مقیاس پارامتر تراوایی (و تخلخل) در مخازن شکافدار استفاده شده است. در ابتدا مدل زمین‌شناسی یک مخزن به صورت شکافدار، سه بعدی و با جریان تک فازی توصیف شده که پارامترهای تراوایی مطلق (و تخلخل) این مدل با استفاده از ترکیبی از توابع موجک هار (Haar)، دابشیز ۴ (Db4) و بایور ۱/۳ (Biro 1.3) افزایش مقیاس یافته است. بدین معنا که در هر مرحله از سه مرحله افزایش مقیاس، از تابع متفاوتی استفاده و در نهایت ۹ مدل افزایش مقیاس یافته، حاصل شده است. استفاده از توابع موجک منجر به افزایش مقیاس هوشمند و غیریکنواخت مدل ریزدانه اولیه می‌شود به طوری که تا حد امکان اطلاعات مهم مدل اولیه مانند اطلاعات اطراف چاه‌ها و همچنین نقاط با تراوایی بالا حفظ شده و سایر نقاط افزایش مقیاس می‌یابد. در این تحقیق استفاده از ترکیبی از توابع موجک منجر به یافتن مدل بهینه افزایش مقیاس یافته، شده است. برای بررسی تأثیر توابع متفاوت موجک در دقت و راندمان مدل افزایش مقیاس یافته، مقادیر عددی چهار پارامتر: سرعت تولید نفت، میانگین فشار مخزن، برش با آب (Water Cut) و مجموع آب تولیدی ۹ مدل افزایش مقیاس یافته، با مقادیر واقعی مدل ریزدانه مقایسه و میانگین خطای پارامترهای فوق محاسبه شده است. این فرآیند در نهایت به یافتن یک مدل بهینه بر اساس زمان شبیه‌سازی و میزان دقت آن در شبیه‌سازی دینامیک یک مخزن سه بعدی شکافدار منتج شده است.

**کلمات کلیدی:** مدل سه بعدی، مخزن شکافدار، افزایش مقیاس، تبدیل موجک، بهینه‌سازی.